

Bundle Binding in Polyelectrolyte Solutions

Mark J. Stevens

Computational Materials Sciences, MS 1111, Sandia National Laboratory, Albuquerque, New Mexico 87185
(Received 27 May 1998)

Stiff polyelectrolytes are found to spontaneously form oriented bundles. Conditions under which bundling occurs are found. Molecular dynamics simulations show that divalent counterions are necessary, and the chains must be sufficiently long and stiff. No aggregation occurs for monovalent counterions. For flexible or short chains, aggregation occurs but bundle formation does not. Because of dynamical constraints, the systems tend to order into a network of connected bundles, not a single bundle. [S0031-9007(98)08120-4]

PACS numbers: 61.25.Hq, 61.20.Ja, 87.15.Nn, 87.15.He

There has been much recent interest in systems of stiff polyelectrolyte systems, because in these systems net attractive interactions occur between the like-charged macroions [1–6]. The general question of when do like-charged macroions attract has much interest, because it is counterintuitive and effects the system structure strongly. Furthermore, DNA is one of the archtypes and thus there are biological implications. Recently, it has been shown that parallel, charged rods can attract due to fluctuations in the counterion distribution [4–6].

In this Letter, simulations of model stiff polyelectrolytes are presented which demonstrate not only aggregation in three dimensions, but also spontaneous bundle formation. The previous works restricted the chain (usually a charged cylinder) center to a plane with the chain perpendicular to the plane. Such restrictions are not put on the chains in this work, and various physical parameters are varied. Specifically, the nature of the aggregate structure is examined for varying chain length (and thus total charge), chain flexibility, monomer density, and counterion valence z_c .

The model used is an extension of earlier polyelectrolyte simulations [7]. The system is modeled as M beadspring chains with N beads. Each bead is charged so that in the model the bond length equals the charge separation along the backbone, $b = a$. The counterions are explicitly treated. All charged particles interact via the Coulomb potential

$$u_{ij}(r) = q_i q_j k_B T \lambda / r, \quad (1)$$

where q_i is the charge on particle i and $\lambda = e^2 / \epsilon k_B T$ with ϵ the dielectric constant of the solution (water). For these simulations we used the particle-particle particle-mesh algorithm to calculate the long-range Coulomb interactions [8,9]. The solvent is modeled by a uniform dielectric background. The Coulomb coupling strength is determined by the Bjerrum length λ . In water at room temperature, $\lambda = 7 \text{ \AA}$. The average charge separation, a is fixed at 1.1σ by the bond potential (see below). The value of $\lambda = 3.2\sigma$ corresponds to $a = 2.5 \text{ \AA}$. Particularly, for divalent ions this is within the counterion con-

densation regime. Most polyelectrolytes have larger radii. For example, DNA has a radius of about 10 \AA . However, the key quantity is the distance of nearest approach of the monomer charge and the solvent ions, and for this distance the diameters are within the physical range. The effect of the monomer radius will mainly be discussed in a future full length paper, and see Ref. [5].

The bond potential is the standard FENE (finite extensible, nonlinear elastic) potential with spring constant $k = 7$, and maximum extent, $R_0 = 2$ [10], where here, as throughout the Letter, Lennard-Jones units are used. All particles interact via a repulsive Lennard-Jones (RLJ) potential with the cutoff at $2^{1/6} d_{\text{ion}}$ where d_{ion} is the ion diameter. The chains are given an intrinsic stiffness by including a bond bending potential, $k_b(\theta - \theta_0)^2$, where $\theta_0 = 180^\circ$ and the spring constant k_b is varied from 0 to 60.

The dynamics of the system is performed at constant temperature, $T = 1.2$, using the Langevin thermostat with damping constant $\Gamma = 1$, and time step 0.015 [11]. For $N = 32$ and 64 at monomer density $\rho = 0.01$, the total integration times are about 4×10^5 and 8×10^5 time steps, respectively. The total simulation time is large enough that chains could diffuse more than the average interchain distance. This is an important issue, particularly for the cases that do not aggregate.

In Fig. 1, we show the most dramatic ordering of the stiff polyelectrolytes for divalent counterions. The chains bind together primarily in two bundles oriented perpendicular to each other. The periodic images show that a connected network of bundles is formed. In the initial configuration the chains were randomly oriented. The bundling is in part due to attraction between two chains due to counterion fluctuations [4–6]. Structures similar to that in Fig. 1 have been observed in experiments on biopolyelectrolytes [3]. This attraction by counterion fluctuation brings two parallel chains together [12]. The present simulations show that pairs of chains also like to aggregate, and that they can align themselves when they are not oriented parallel. Aggregation occurs quite generally with multivalent counterions. As discussed below,

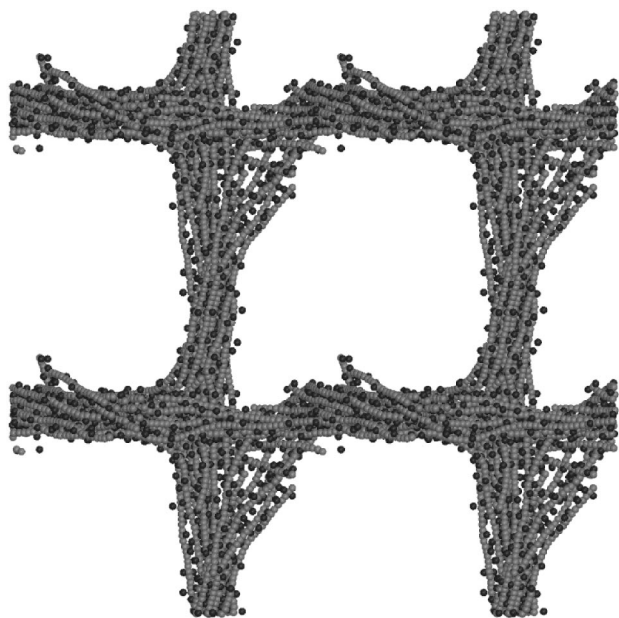


FIG. 1. Bundle configuration of $N = 64$, $M = 16$, $k_b = 60$, and $z_c = 2$ system at $\rho = 0.01$. The figure shows four periodic images in order to exhibit the connecting chains between bundles; there are only two bundles in the simulation cell. The counterions are the dark spheres and the monomers are the light spheres.

aggregation occurs independent of chain lengths and intrinsic stiffness. On the other hand, bundle formation depends on these parameters, and there tends to be frustration of ordering into a single bundle.

In general, the initial aggregation occurs rather quickly. However, ordering within aggregates is slow, because chain motion is strongly constrained by other chains. A chain in a bundle must reptate along its backbone taking much longer to diffuse. The total system energy decreases slowly once the system has aggregated. The average system energy reaches a constant value in all the simulations. For systems that form bundles, a minimum energy is reached once the system has organized into multiple bundles and is stable for several hundred thousand time steps. The energy of a system forming a single bundle is lower than the multibundle state. It is clear that the multibundle state is metastable and any transition would occur only after a long time. Chains within a bundle are strongly bound to each other, as will be demonstrated. A transition of a chain from one bundle to another is extremely slow. The chain dynamics in these simulations imply that transformations of two bundles into one will take orders of magnitude longer than the total simulation times performed here. Thus any transition to a single bundle is beyond the capabilities of the present simulations.

Even at low densities constraints on the chain dynamics frustrate bundling. In particular, consider two chains that overlap at some point. For example, they cross to form

an “X”. A third chain randomly placed near the first two will likely end up between one set of the legs of the X and not in the plane of the X. The two chains in the X cannot become parallel without the chain between them moving out of the way. Such dynamics is seen in these simulations. Another typical constraint at densities above overlap is that multiple bundles form and the ends of chains in one bundle are connected to two others (e.g., Fig. 1). There is then no preferred direction for the chains to move in order to reduce the number of bundles. The chains are likely to oscillate within their bundle for long times before moving to another bundle.

We now describe the nature of the system structure as various parameters are varied. Figure 2 shows the interchain monomer-monomer radial distribution function, $g_{mm}(r)$. A very large peak occurs at $r = 2$ due to the presence of an ionic triplet [13] where a divalent ion is between two monomers on separate chains. The peak height monotonically increases with the chain length, or equivalently, the total chain charge. This is consistent with the expectation that the attraction between chains grows with total charge. For the two larger chain lengths $N = 32$ and 64 , a shoulder exists at $r = 4$, due to ionic quintuplets. Thus, there are many sets of ionic quintuplets connecting 3 chains for these N . The Coulomb energy of just the ions of an ionic triplet is $-11.2k_B T$. Such a large negative energy suggests that the ionic triplet would be very stable in comparison to a free counterion, and that a pair of chains containing many ionic triplets are even more strongly bound to each other. Note that within a bundle a counterion need not be bound to a monomer to possess the energy of an ionic triplet. The counterion

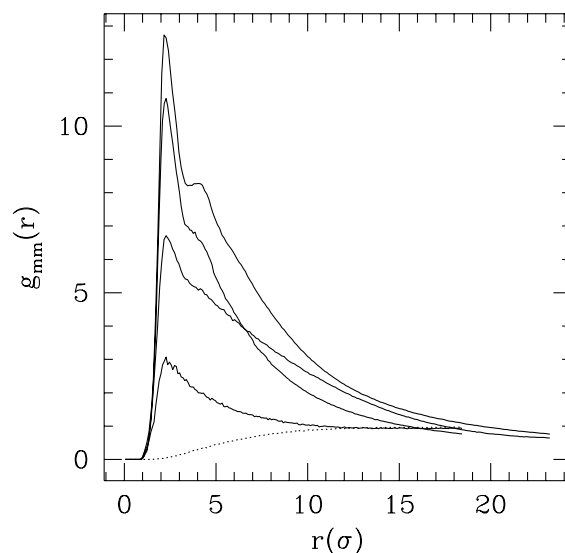


FIG. 2. The interchain monomer-monomer radial distribution function as a function of chain length for $\rho = 0.01$. From largest main peak to smallest, the chain lengths are 64, 32, 16, and 8 for $z_c = 2$ (solid lines). The dotted line is for $N = 32$ and $z_c = 1$.

can move between two parallel chains and still be in an ionic triplet. Trajectories show this occurs. In fact, the counterions diffuse rapidly in comparison with the chains as they move unimpeded within the bundle network.

An indication of the change in the system order is the crossover of g_{mm} between $N = 16$ and $N = 32$ at $r \approx 7$. This implies that at $r > 7$, one is more likely to find a pair of monomers on separate chains at $N = 16$ than $N = 32$. If all the chains were in a bundle of radius r_b , then for $r > r_b$ the $g_{mm}(r)$ would be zero. On the other hand, if the chains aggregate, but do not bundle, then $g_{mm}(r)$ will decay more slowly. The g_{mm} data imply that the aggregation of the chains yields a tighter, more bundled structure as N increases.

Divalent ions are critical for the aggregation. Figure 2 shows the $g_{mm}(r)$ for $N = 32$ and monovalent counterions. In contrast to the peak present in the divalent systems, the monovalent g_{mm} exhibits a correlation hole indicating the chains effectively repel each other. This is consistent with the body of literature which finds that divalent ions are necessary for short-range attraction between like-charged macroions [5,6,14,15]. For monovalent ions attraction could occur, but the counterion diameter would have to be unphysically smaller.

The number of counterions “condensed” on the chains in divalent solution is extremely large and clearly drives the aggregation. The distance between a counterion and a chain is calculated as the minimum of the distances between the counterion and all the monomers of the chain [16]. The number of condensed counterions, n_c , is taken to be the average number of counterions within 1.5σ of the chain. For the system in Fig. 1 n_c is $0.80N$. Given the counterions are divalent, the amount of charge near a chain is $1.6N$; there is overcharging of single chains. To attain a charge greater than N depends on the sharing of the counterions among multiple chains. Overcharging of the chains yields chain-chain attraction and aggregation. For $N = 32$ and 16 , $n_c = 0.78N$ and $0.67N$, respectively. Even for the $N = 8$, $n_c = 0.56N$ yields a counterion charge greater than N . These results are consistent with the peaks present in Fig. 2.

The orientational order in the system can be determined by examining the following correlation function. Let \hat{n}_i be the unit vector in the direction of the end-to-end vector, \mathbf{R} for the i th chain. A correlation function that indicates the presence of nematic ordering is the second order angular correlation function in the spherical harmonic expansion [17]

$$g_{220}(r) = 1 + \frac{5}{2} \frac{\langle \sum_{i \neq j} \delta(r - r_{ij}) [3(\hat{n}_i \cdot \hat{n}_j)^2 - 1] \rangle}{4\pi\rho Mr^2}. \quad (2)$$

This function is chosen over the other second order functions, because it is a function of \hat{n}^2 so that the sign of \hat{n} is unimportant as it is in this case. The position r is taken to be the position of the middle monomer.

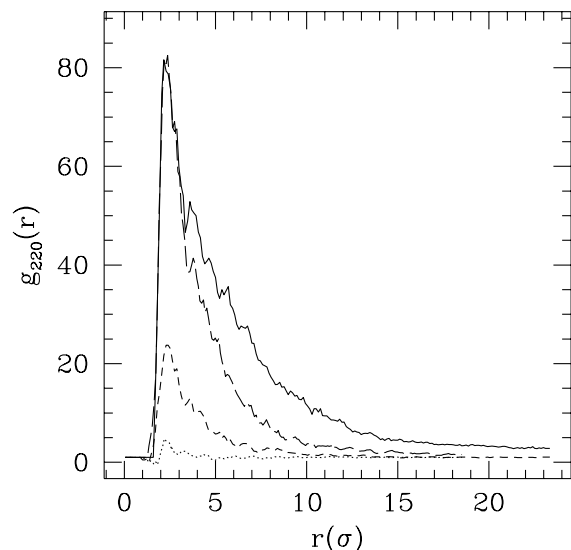


FIG. 3. The g_{220} radial distribution function as a function of chain length for $\rho = 0.01$ and $z_c = 2$. The chain lengths are $N = 64$ (solid line), 32 (long-dashed line), 16 (short-dashed line), and 8 (dotted line).

A maximum occurs when chains are aligned parallel. Figure 3 shows a plot of g_{220} for the same divalent systems as Fig. 2. The data are noisier than in Fig. 2, because here the number of contributions is M^2 instead of $(NM)^2$. Nonetheless, the $N = 64$ and 32 show very large peaks at $r = 2$ due to pairs of chains being strongly aligned. The correlated order between chains does not decay for these N until large chain separations ($r \geq 10$) corresponding to the size of the bundles. However, as N decreases and r increases, the alignment disappears. Thus, bundling requires sufficiently large N .

We have seen that bundling occurs for stiff, long chains, and when the chain length decreases, the degree of bundling decreases. Presumably, the same will happen as the chain stiffness decreases. Particularly for divalent counterions in the condensation regime, the screening of the monomer-monomer Coulomb repulsion will be strong. A fully flexible chain is as coiled as a neutral chain [18]. Figure 4 shows g_{mm} for a range of k_b . Aggregation occurs even for $k_b = 0$, but between $k_b = 20$ and 3 a qualitative change occurs in the form of g_{mm} . For the stiffer chains the initial peak is higher, occurs at the ionic triplet separation, and decays faster beyond the bundle width. For the floppier chains the peak becomes very broad and shifts to larger r . A flexible chain can form ionic triplets between its own monomers, thus shielding monomers from other chains and shifting the peak in g_{mm} . Examination of configuration images shows that at $k_b = 20$ subsets of chains form bundles which then are connected to other similar bundles to form a fibrous three-dimensional network structure. At $k_b = 3$, bundles do not form at all. Instead the chains aggregate into a “hairy” mess.

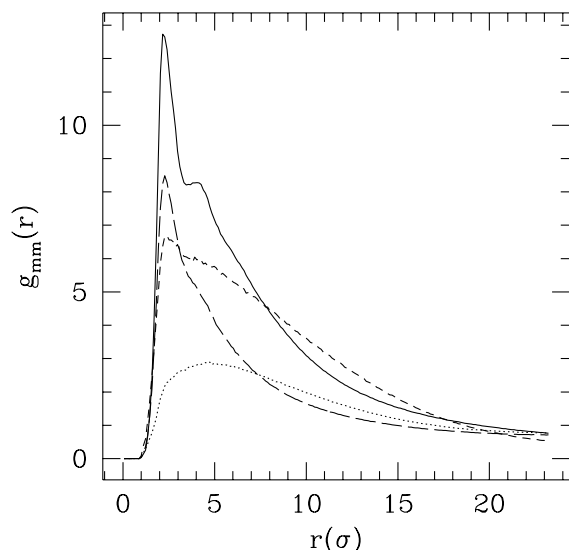


FIG. 4. The interchain monomer-monomer radial distribution function as a function of k_b for $N = 64$, $\rho = 0.01$, and $z_c = 2$. From largest main peak to smallest, the k_b are 60 (solid line), 20 (long-dashed line), 3 (short-dashed line), and 0 (dotted line).

Since these systems aggregate, it is natural to ask whether phase separation would occur. The osmotic pressure for the aggregating systems is very small and in some cases the average is negative. A negative pressure would imply that the phase point is in a coexistence region. Such coexistence regions have been predicted for systems with multivalent counterions [19,20]. The sign of the pressure is not that significant. If the magnitude is very small, then it is likely to be smaller than the pressure at very dilute concentrations which will approximately be $\rho k_B T$. In that case, there must be a van der Waals loop and coexistence in the equilibrium phase diagram. To test this point requires a different set of calculations such as constant pressure simulations. A few constant pressure simulations [21] have been performed on the larger systems. The system contracts to the density of 0.1 which is that within the bundles. In the process of contracting, the multiple bundles merge, but do not orient. Again, it may become an oriented bundle, but only on time scales way beyond what can be simulated.

Another important issue is the system size, particularly the number of chains, M , in the simulations. For the present set of simulations one cannot determine the structure of the bundle network that occurs for the longer chains. For $N = 8$ and 16, there is not much concern since $M = 64$ for these smaller chains. In these cases, the cell length is larger than the chain length. Even the aggregate does not span the cell. The Coulomb interactions outside the aggregate are strongly screened. For aggregates that do not span the simulation cell, the system sizes are clearly

sufficient. However, for the larger chains at the high densities such as in Fig. 1, the situation requires more testing. For $N = 32$ and 64 with $M = 16$ at $\rho = 0.01$, the chain lengths are longer than the cell length. Simulations were performed for $N = 32$ and 50 with $M = 50$ to achieve cell lengths greater than the chain lengths. The data for these simulations are consistent with the smaller systems' data (i.e., Figs. 2–4). Moreover, the tendency for multiple bundles to form is even more pronounced.

The seemingly odd phenomenon of attraction between like-charged polymers is already well founded [1,5,6,14,15] and further confirmed here. The present work shows that under the right circumstances ordered structures can result and the dynamics of the interactions are important because metastable states easily occur. In particular, stiff chains can spontaneously orient themselves into multiple bundles. The bundles tend to form a network superstructure, because their motion is highly constrained.

-
- [1] L. Guldbrand, L. Nilsson, and L. Nordenskiöld, *J. Chem. Phys.* **85**, 6686 (1986).
 - [2] V. Bloomfield, *Biopolymers* **31**, 1471 (1991).
 - [3] J. Tang, S. Wong, P. Tran, and P. Janmey, *Ber. Bunsen-Ges. Phys. Chem.* **100**, 1 (1996).
 - [4] J. Ray and G. Manning, *Langmuir* **10**, 2450 (1994).
 - [5] N. Grønbech-Jensen, R. Mashl, R. Bruinsma, and W. Gelbart, *Phys. Rev. Lett.* **78**, 2477 (1997).
 - [6] B.-Y. Ha and A. Liu, *Phys. Rev. Lett.* **79**, 1289 (1997).
 - [7] M. Stevens and K. Kremer, *J. Chem. Phys.* **103**, 1669 (1995).
 - [8] R. Hockney and J. Eastwood, *Computer Simulation Using Particles* (Adam Hilger, New York, 1988).
 - [9] E.L. Pollock and J. Glosli, *Comput. Physics Commun.* **95**, 93 (1996).
 - [10] B. Dünweg and K. Kremer, *Phys. Rev. Lett.* **66**, 2996 (1991).
 - [11] T. Schneider and E. Stoll, *Phys. Rev. B* **17**, 1302 (1978).
 - [12] B.-Y. Ha and A. Liu, report, 1998 (to be published).
 - [13] The term ionic triplet is introduced to distinguish the state from an ion bridge in which the counterion is fixed in position.
 - [14] R. Kjellander and S. Marčelja, *Chem. Phys. Lett.* **112**, 49 (1984).
 - [15] M. Stevens and M. Robbins, *Europhys. Lett.* **12**, 81 (1990).
 - [16] M. Stevens and S. Plimpton, *Eur. Phys. J. B* **2**, 341 (1998).
 - [17] J.J. Weis and D. Levesque, *Phys. Rev. E* **48**, 3728 (1993).
 - [18] M. Stevens, report, 1998 (to be published).
 - [19] M.O. de la Cruz *et al.*, *J. Chem. Phys.* **103**, 5781 (1995).
 - [20] J. Wittmer, A. Johner, and J. Joanny, *J. Phys. II (France)* **5**, 635 (1995).
 - [21] G.S. Grest, M.D. LaCasse, K. Kremer, and A.M. Gupta, *J. Chem. Phys.* **105**, 10583 (1996).